



# A Step Toward Proposing a Force Reduction Factor for Hybrid GFRP/Steel Reinforced Concrete Columns Under Earthquakes

Ahmed Arafa<sup>a\*</sup>, Marwa Hesham<sup>a</sup>, Mohamed M. A. Hussein<sup>a</sup>

<sup>a</sup>*Civil Engineering Department, Faculty of Engineering, Sohag University, Sohag, 82524, Egypt*

---

## Abstract

The use of hybrid reinforcement (Steel/GFRP) system was proposed in the present study as a vital solution for overcoming corrosion problem with a proper energy dissipation capacity. This study also presents a preliminary step toward developing a force reduction factor for concrete columns reinforced with hybrid reinforcement. Nonlinear finite-element analysis (FEA) was used as a tool to achieve the research target. A novel FEA model for RC columns that captures the behavior of concrete columns solely reinforced with steel or GFRP bars and have been previously published by the first author, was first summarized. The study was then extended to test the effect of using hybrid reinforcement in terms of crack patterns, failure modes and load–lateral displacement hysteretic response. The force reduction for the hybrid RC specimen was also estimated. The reported test results clearly revealed that properly detailed hybrid RC columns have a recoverable and self-centering ability. The hybrid RC column sufficiently achieved the maximum drift meeting the limitation of most building codes. Acceptable levels of energy dissipation accompanied by relatively small residual forces, compared to the steel-reinforced column, were observed. The force reduction factor was suggested to be taken 2.5 for hybrid RC columns.

© 2023 Published by Faculty of Engineering – Sohag University. DOI: 10.21608/SEJ.2023.232799.1044

Keywords: Seismic design, force reduction factor, ductility, drift capacity, hybrid reinforcement (steel/GFRP).

---

## 1. INTRODUCTION

Corrosion of steel reinforcement in concrete structures constitutes a major durability problem that leads to structural degradation and costly repairs. This is typically true under the direct exposure to freeze–thaw cycles, deicing salts in winter months as well as the coastal weather. Annually, thousands of infrastructure buildings are in need of repair and rehabilitation or complete replacement, which constitutes a serious problem when measured in terms of rehabilitation costs and traffic disruption [1]. As a viable solution for the problem the fiber reinforced polymer (FRP) bars are now required in new reinforced concrete due to their non-corrosiveness, lightweight, and high strength. Numerous studies have been done to examine how well FRP bars function on various structural components like slabs, beams, and columns. Improvements in the behavior of the structural elements were discovered, and design equations for such elements under the effect of dead and live loads were provided in the ACI 440.1R [2] and the CSA S806 [3]. Additionally, researchers conducted experiments to check the effectiveness of FRP bars in region exposed to earthquakes. The experiments included different earthquake resisting structural elements such as columns, beam–column connections, and shear walls Arafa et al. [4]. The test specimens showed elastic behavior with negligible damage and minimal strength decay, whereas the failure was brittle. In the seismic design, the design seismic force is lower than the equivalent lateral force representing elastic response by a force modification factor. The factor is taken to reflect the structure’s ductility, showing its capability to dissipate energy through inelastic behavior. Considering the lack of ductility in FRP RC elements, the different FRP design codes and guidelines specify that the force reduction factor is equal to unity. This made the use of FRP RC elements is proper in regions that experience frequent regular, low-amplitude earthquake activity [5] in which the direct equipment of structure after earthquakes is necessary. Whereas in places with rare strong earthquakes, huge sections with substantial reinforcement will be required when constructing the structural elements in the elastic stage. This will result in an unprofitable design. Because steel bars give the structure ductility, which in turn helps to disperse and lessen seismic power, researchers [6-13] resorted to creating the structural elements using hybrid reinforcements of steel and FRP bars. As result, the design would be cost-effective, and a reasonable force

---

\* Corresponding author: [ahmed\\_arafa@eng.sohag.edu.eg](mailto:ahmed_arafa@eng.sohag.edu.eg)

reduction factor can be received. Between many methods that have been proposed in this aspect, Arafa et al. [13] studied this idea using reinforced concrete columns with hybrid reinforcement, where GFRP bars served as the primary reinforcement and steel bars were added at inner layer away the weather circumstances. The columns had a great capacity for dissipating energy with minimal damage. The present study is a continuation the step started in the reported paper by estimation the force reduction factor for hybrid RC columns. The previously built model was first presented. This is followed with modeling a hybrid RC columns and discussion considering the new behavior of cracks, ductility, residual damage, as well as estimating the force reduction factor.

## 2. FEA NUMERICAL MODEL AND VALIDATION

Arafa et al. [14] built a numerical analysis that can capture the cyclic behavior of concrete columns reinforced with either steel, or GFRP bars. Specialized 2-D finite-element program (VecTor2) was used in the modeling. In the literature [15-17], it is well established that the finite element model (FEM) developed for structural elements reinforced solely with steel or FRP bars can accurately predict the behavior of hybrid reinforced elements. Considering these findings, and due to the lack experimental results, the FE model built by Arafa et al. [14] was adopted in the present study. A brief summary for the model is presented in the following subsections. This is followed with a numerical study on hybrid RC column.

### 2.1 The FEA Model Description

The FEM was built and validated based on the experimental results of one well-detailed GFRP-reinforced, and one steel RC columns in the literature [18]. The specimens had a cross section with dimensions of 400 mm × 400 mm and a height of 1650 mm. The columns were tested under reversed cyclic lateral loading applied at the columns tip, while simultaneously subjected to axial load representative to the dead and live load on the structure (Fig. 1). Table 1 lists the specimens details and gives the actual concrete compressive strength based on the average values from tests performed. The tested axial load ratio (ALR) was equal to 20% that is defined using this equation  $P/f_c'A_g$ , where  $P$  is the constant axially applied compression load,  $f_c'$  is the concrete compressive strength, and  $A_g$  is the gross cross-sectional area of the column. Table 2 shows the material properties of the reinforcing bars.



Fig. 1. Test setup (Elshamandy et al. 2018).

TABLE 1. TEST SPECIMEN DETAILS

Specimen ID	$f_c'$	$\rho_l$ , %	Transverse reinforcement	
			$\rho_v$ , %	$s$
Steel RC column	34	0.53	0.5	100
GFRP RC column	39	0.95	0.71	100

Notes:  $f_c'$  is concrete compressive strength (MPa);  $\rho_l$  is longitudinal reinforcement ratio;  $\rho_v$  is transverse reinforcement ratio;  $s$  is spacing of transverse reinforcement (mm);  $P/f_c'A_g$  is axial load level;  $EA$  is axial stiffness;  $E$  is longitudinal bar modulus of elasticity.

TABLE 2. MECHANICAL CHARACTERISTICS OF THE USED REINFORCEMENT

Bar*	$d_b$ , mm	$A_s$ , mm <sup>2</sup>	$E_f$ , GPa	$f^{\dagger}, f^{\ddagger}$ , MPa	$\epsilon_{f/it}$ , %
Straight bars					
9.5	71.3	200	$f_y = 420$	$\epsilon_y = 0.2$	9.5
12.7	126.7	69.6	1392	2.00	12.7
Bent GFRP N10 (No. 3) rectilinear spiral and crossies					
Straight	9.5	71.3	52	962	1.85

\*Numbers in parentheses are manufacturer's bar designation.

Four-node quadrilateral elements were used in the developed FE model to model the concrete, while the longitudinal bars were represented explicitly by truss elements. Fig. 2 shows a representative finite element mesh and set of truss elements used in the analysis. The confinement stirrups were simulated as smeared reinforcement in order to shorten the solution process time and avoid convergence problems. The hysteretic response, failure mode, ultimate strength, and drift ratio were examined for the simulated columns with different mesh sizes and compared to the experimental test results. Fixation against movement in both the horizontal and vertical directions was select for the nodes at the base to simulate the real case at the laboratory. The lateral displacement was applied at a height of 1650 mm from the base. The adopted constitutive models used in modeling the concrete, reinforcement and the bond between them are listed in Table 3.

- Reinf. 1: 3 #3 straight GFRP or steel bars.
- Reinf. 2: 2 #3 straight GFRP or steel bars.
- Conc. 1: Heavy reinforced concrete
- Conc. 2: Normal reinforced concrete
- Conc. 3: Concrete reinforced with smeared stirrups

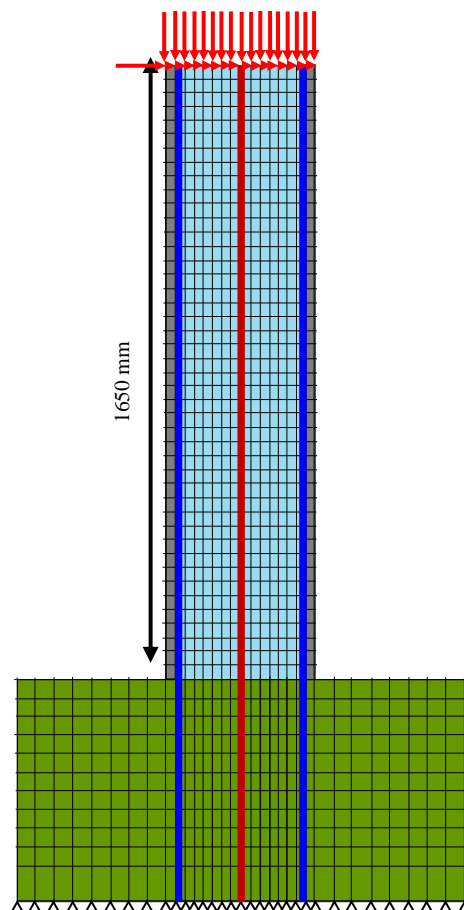


Fig. 2. Typical FE meshing (Arafa 2021)

TABLE 3. CONSTITUTIVE MODELS USED IN THE FE ANALYSIS

Models	Parameter	Models used in FE analysis
Concrete	Hysteretic response	Palermo and Vecchio with decay [19]
	Concrete compressive pre- and post-peak response	Hognestad [20] and modified Kent–Park formulation [21]
	Slip distortion	Vecchio-Lai model [22]
	Tension stiffening	Bentz model [23]
	Confinement strength	Kupfer-Richart model [24]
	Dilation	Variable-Kupfer [24]
	Cracking criterion	Mohr-Coulomb (stress)
FRP bars	Hysteretic response	Elastic
	Dowel action	Omitted as proposed by ACI 440.1R [2]

## 2.2 The FEA Model Verification

Figure 3 compares the experimentally reported and the corresponding analytically predicted cracks pattern and failure modes of representative tested column. Generally, the simulated columns exhibited crack patterns like those recorded in the experiments representing crack inclination, trends, and propagation. The reported simulation results (Fig. 3) also demonstrated the ability of FEA in predicting the experimentally observed failure modes. The failure was mainly controlled by concrete crushing as flexural behavior dominated the response. This was associated with sequential fracturing of the compressed longitudinal bars and subsequent rupture of the transverse reinforcement.

Figure 4 plot the analytical and experimental load–drift hysteric response ratio. The figures clearly show that the FEA model predicted well the main features of the experimental hysteric response in terms of strength, stiffness, and deformation capacities. The numerical model captured the pinched behavior in the hysteric response of the GFRP-reinforced column, which was induced by the elastic nature of the GFRP bars, while wide loops for the steel RC column induced by the ductility of steel. An initial linear branch—corresponding to the uncracked condition of the columns—was evident. The FE model also predicted the experimental ultimate strengths with very high accuracy, that is, to within 3%. The model slightly underestimated the experimental ultimate drift ratios since the difference was within 12%. The slight difference between the predicted and experimental ultimate drift ratios can be attributed to the bond model, which seems to underestimate the bond degradation at failure.

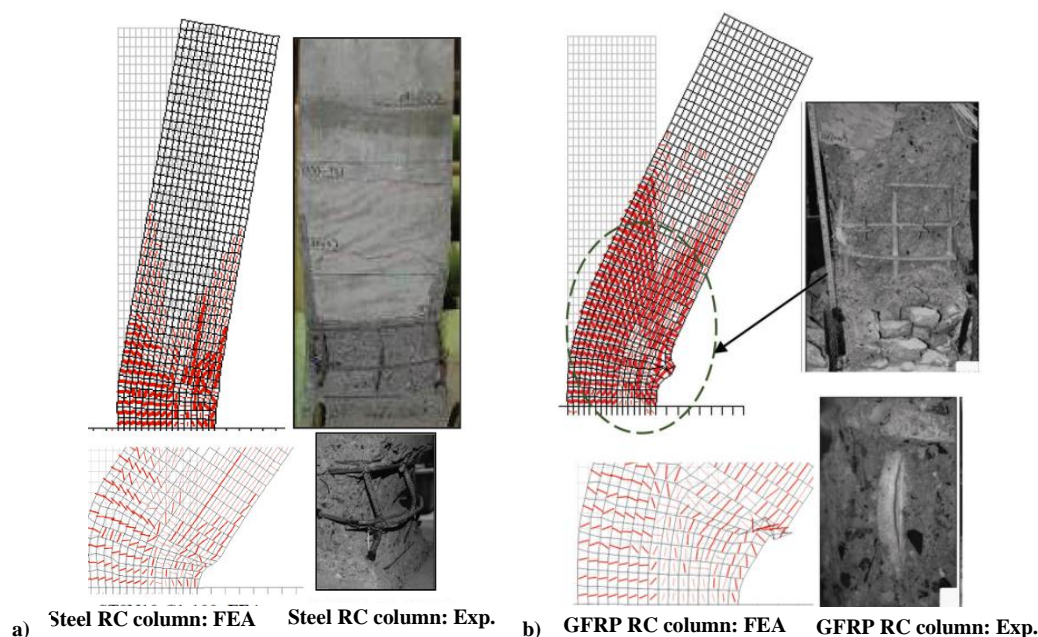


Fig. 3. Cracks pattern, and failure mode obtained from experimental and FEA results for: a) Steel RC column; and (b) GFRP RC column (Arafa et al. 2021).

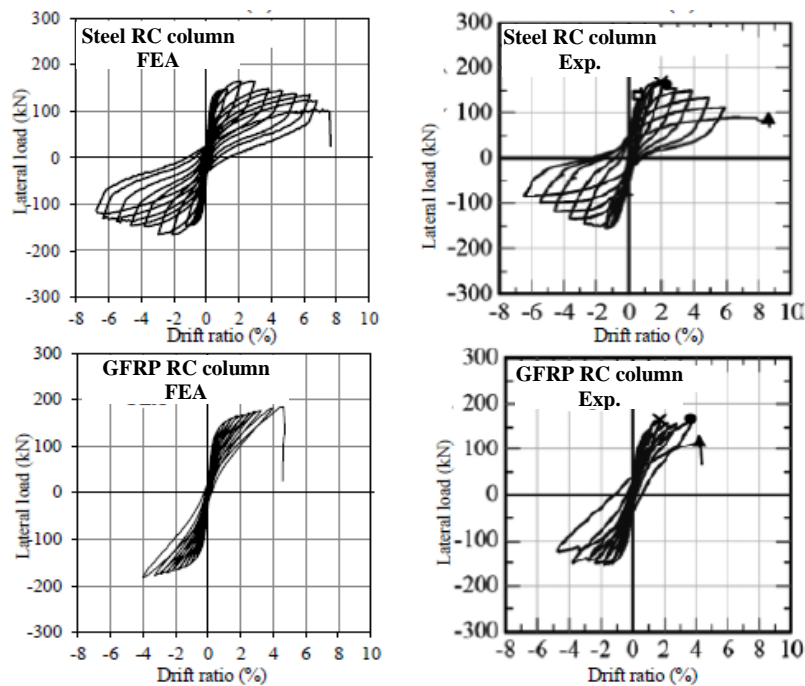


Fig. 4. Load drift ratio hysteretic response (data of modeling GFRP RC from Arafa 2021).

### 3. HYBRID REINFORCEMENT (STEEL/GFRP) SELECTION

Two main issues were considered in nominating the hybrid reinforcement systems. The first issue is the location of steel and FRP bars. This should be carefully selected such that achieving the best functionalities of this system and accomplish the specified aims. In this context, it is well known that the reinforcement closer to the concrete cover is the most vulnerable to corrosion because of bidirectional corrosion and the rapidly spalling concrete cover at this site. Accordingly, and with aim of achieving a high level of durability and corrosion resistance for the concrete column, the steel bars will be placed in an inner layer with a thicker concrete cover, while the FRP bars will be the out layer to be the line of defense against corrosion. The second point is achieving high level of ductility before concrete crushing or FRP rupture, while achieving stiffer behavior. Accordingly, localizing the steel bars close to the maximum strain in both sides will be the most effective location for this target. Considering the two points, the present study included three specimens, one reference specimen reinforced with GFRP that have been previously described (Arafa et al. 2021)[14], and two more specimens (steel RC column, hybrid RC column) that have been designed to give almost the same strength of the reference GFRP RC specimen. The cross section with reinforcement details for three specimens is shown in Fig. 5. The mechanical characteristics of the used reinforcement are listed in Table 4.

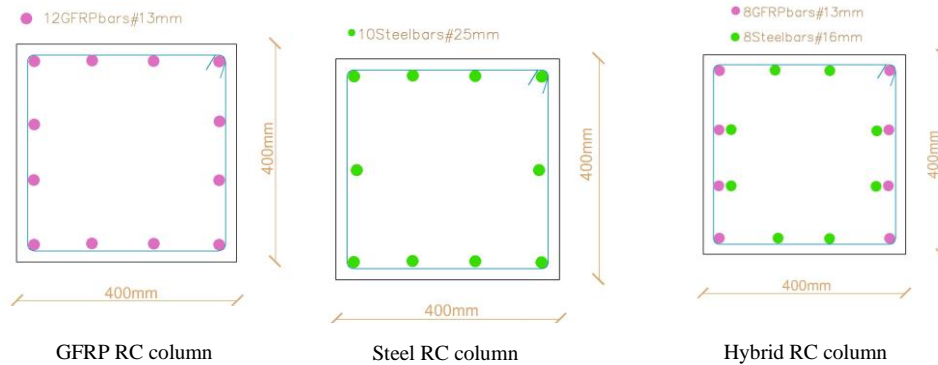


Fig. 5. Geometry and reinforcement details of the simulated specimens.



TABLE 4. MATERIAL PROPERTIES

Bar	Designated Bar Diameter (mm)	Nominal Area <sup>1</sup> (mm <sup>2</sup> )	Tensile Modulus of Elasticity <sup>2</sup> (GPa)	Tensile Strength <sup>2*</sup> (MPa)	Average Strain at Ultimate (%)
No. 10 GFRP	9.5	71	65.1	1372	2.1
No. 13 GFRP	12.7	126.7	65.6	1312	2.0
Steel No. 25	25	491	200	$f_y = 420$	$\epsilon_y = 0.5$

## 4. TEST RESULTS AND DISCUSSION

### 4.1 Cracks Pattern and Failure Mode

The failure mode and cracks pattern of the simulated specimens are depicted in Fig. 6. The specimens exhibited initial rigid behavior without cracks. Flexural cracks that start at the bottom of the column are significantly reduced in lateral stiffness as force increases. As the load increases, cover cracking and slow concrete cover spalling started at the most squeezed fibers of the columns. This was recorded from the measured concrete compressive strain, which peaked at 0.0035 at the base of the columns and then spread upward. After that point, the simulated specimens exhibited differently. The steel RC columns exhibited yielding of steel bars with subsequent mobilizing the deformation at the plastic hinge zone and noticeable damage. This is clear from Fig. 6a, where the cracks and damage localized close to the column base. The failure of specimen occurred due to concrete crushing at the column compressed toe with abrupt strength drop. For the GFRP RC columns, the scene was completely different, where the damage was insignificant, and the cracks almost vanish at zero loading. This attributed to the elastic nature of GFRP bars that get the structure back to the origin after loading. The specimen kept carrying the load without losing strength. In contrast the steel RC column, the cracks in the GFRP RC distributed along the wall height. The cracks, however, at the maximum load in any the cycle was wider than the steel RC column that is associated to the lower modulus of the GFRP bars compared to steel bars. At the end, the GFRP RC column showed sudden strength reduction and bars ruptures at the most tensile fiber as shown in Fig 6b. The figure makes it is obvious that meshes in the tension zone exhibit substantial vertical deformation, which suggests that bars have ruptured. The hybrid RC columns showed modest behavior between that described for the steel and GFRP RC columns (Fig. 6c). The cracks are tighter than the GFRP column due to the high steel bars modulus. The cracks distributed at longer zone than the steel, hence the damage was distributed and alleviated. Due to the existence of GFRP bars, the cracks tended to close between load reversals with minimal residual deformation as well be discussed later. The steel bars yielded and gained the structure with ductility, while the GFRP gain the structure with elasticity as the load vanish. Additionally, the specimens exhibited steady behavior with no strength degradation up to failure. Compression failure due to concrete crushing distinguished the specimen failure.

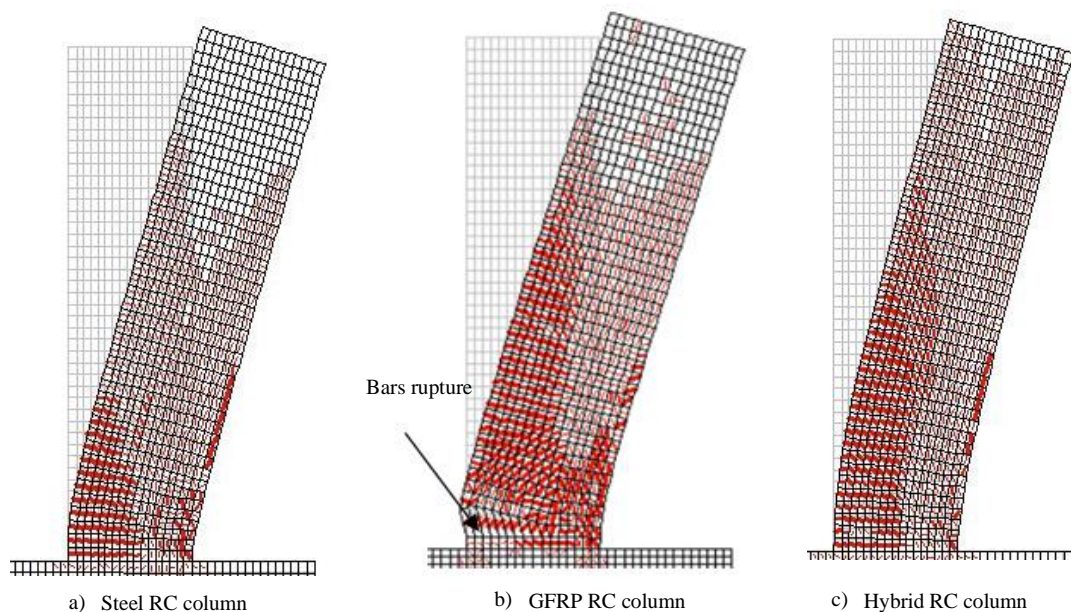


Fig. 6. Cracks pattern and failure mode for the simulated specimens

#### 4.2 Load-Drift Hysteretic Response and Energy Dissipation

Fig. 7 compares the load-drift ratio hysteretic response of the simulated specimens. Generally, the steel RC showed wider loops than its companions, but with noticeable damage after the yielding point. In the GFRP RC column, the loops were tight due to the elastic nature of GFRP bars. In between, the hybrid RC column exhibited wide loops due to steel yielding, while the residual damage is much lower than steel RC specimen due to the role of GFRP column. This behavior is reflected on the measured cumulative energy dissipation for the three specimens and shown in Fig.8. Noticeably, the existence of steel bars enhanced the energy dissipation, albeit lower than the steel RC column.

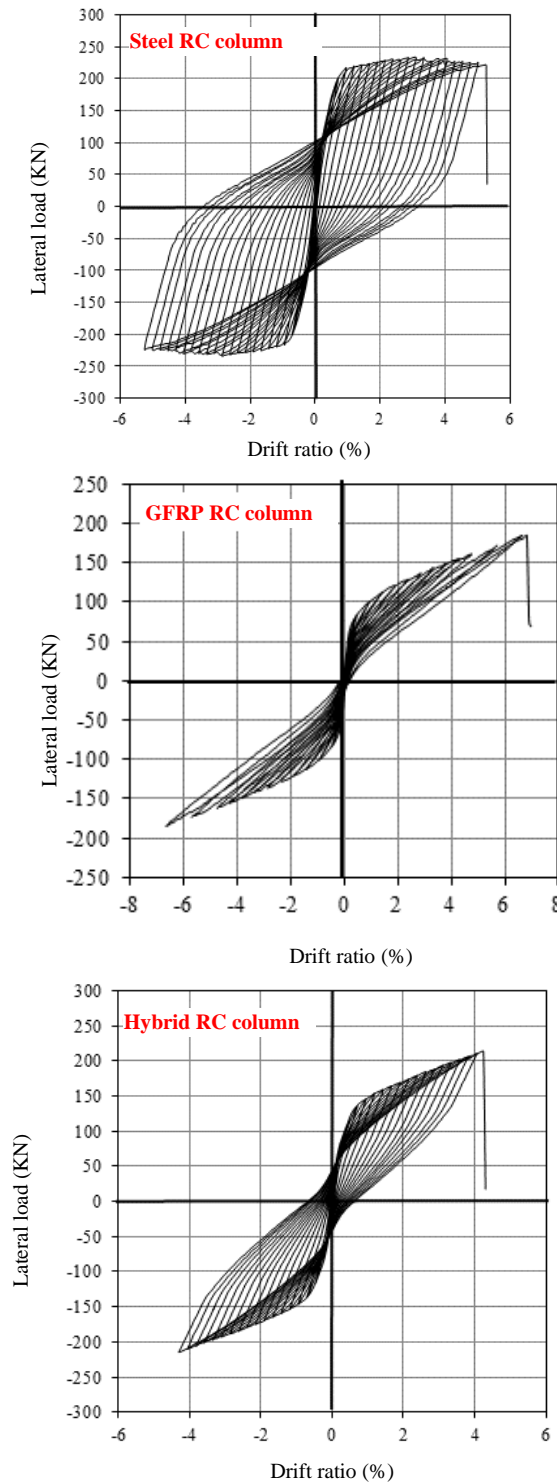


Fig. 7. Failure mode and Hysteretic response.

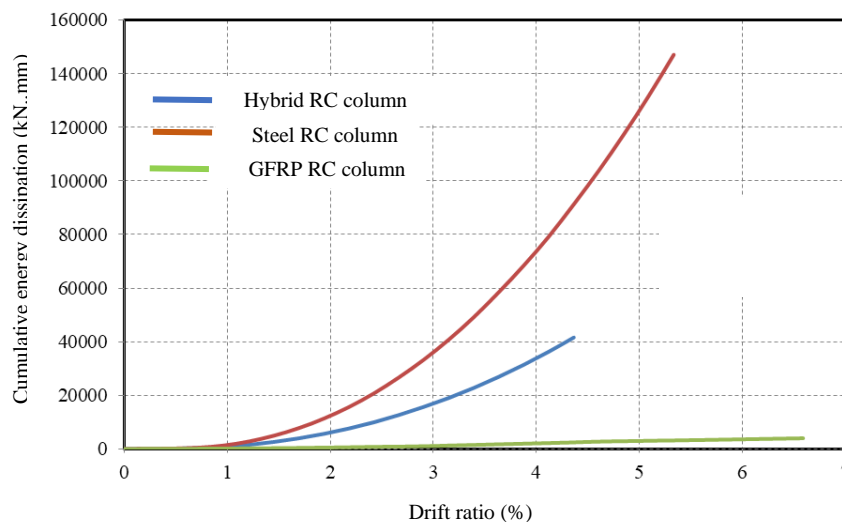


Fig. 8. Cumulative energy dissipation versus drift ratio.

#### 4.3 Envelope curves response

Fig. 9 compares the load-drift ratio envelope curves for the steel, GFRP, and hybrid RC columns. All specimens exhibit comparable initial stiffness up to the onset of the first flexure crack. After this stage, the reinforcement type differentiate behavior. The hybrid RC column responded more stiffly than the GFRP RC columns due to the high modulus of elasticity of steel bars in comparison to GFRP bars. This would be preferable in the design under frequent low or moderate earthquake as the displacement demand would be lower with no damage to the non-structural elements. The hybrid RC columns showed comparable ultimate strength to the GFRP RC specimens, as was intended in the design. Another thing that can be deduced from Fig. 9 is that the hybrid reinforcement system seems to lower the final drift ratio. This is predicted and is associated to the bond slip between concrete and FRP is alleviated with the existence of steel bars. Moreover, the failure mode of hybrid RC column is compression failure that accelerated the failure occurrence.

It should be noted that the acceptance criteria of the National Building Code of Canada (NBCC) [25] requires that the columns should be able to retain its structural integrity and at least three-quarter of its ultimate capacity through peak displacements equal to or exceed a story drift ratio of 2.5%. All tested specimens were successfully able to sustain drift ratios higher than the values required by NBCC.

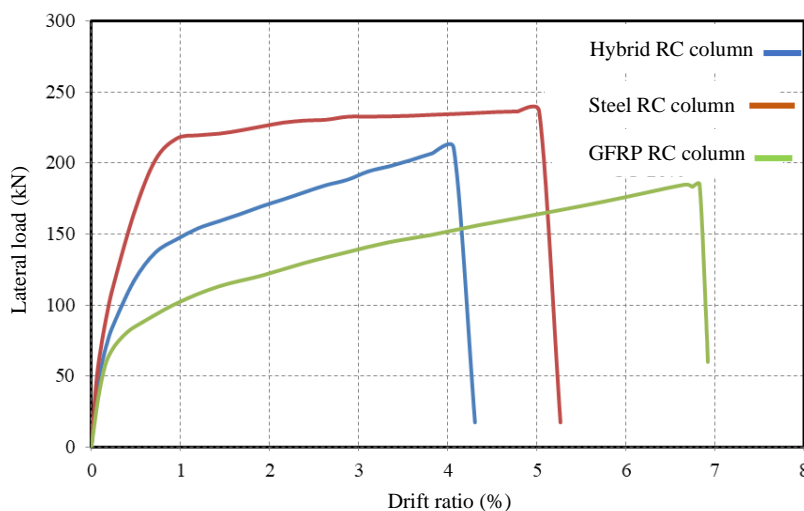


Fig. 9. Cumulative energy dissipation versus drift ratio.



#### 4.4 Residual Displacement

Fig. 10 shows the lateral drift ratio versus the residual displacement as indicator for the residual damage as borne out by many research groups [26-29]. The GFRP RC column sample has very little residual damage because of the flexible nature of the GFRP bars. In contrast, the steel RC column exhibited significant damage which entails necessitating expensive repairing process. Further, it can be observed that the residual damage was significantly controlled in the hybrid column sample compared to the steel RC column, which is the goal of the design. Little damage occurs that permit the ductility with a reasonable reduction factor, while the repairing will be affordable.

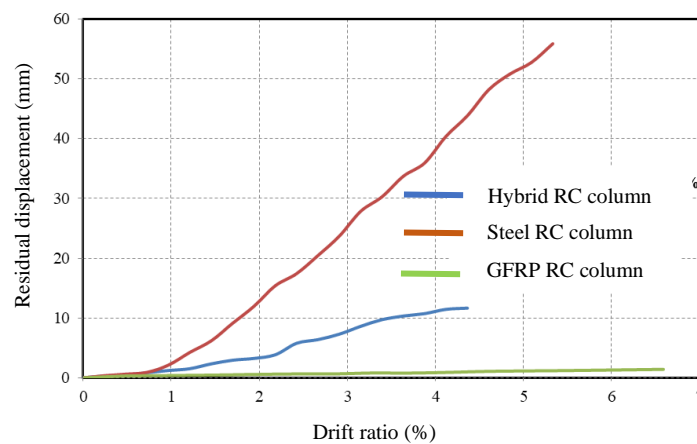


Fig. 10. Cumulative energy dissipation versus drift ratio.

#### 4.5 Ductility Factor

A big challenge in the use of hybrid RC column is achieving high level of ductility: i.e, the yielding point occurred before the GFRP bars rupture in the tension side or the concrete crushed at the compression zone. To check this point, the ductility index, measured as the ratio of ultimate displacement to yield displacement, was calculated for the simulated specimens and plotted in Fig. 11. As shown, the ductility index was equal to 4.8, 5.9 for the hybrid, and steel RC columns, respectively. More specific, it can be said that the hybrid specimen achieved a satisfactory ductility factor that is almost 80% the value achieved by the steel RC column. Hence the replacement of GFRP with some steel bars is effective in lending the structure with ductility that is surely important in the context of reducing the seismic force demand.

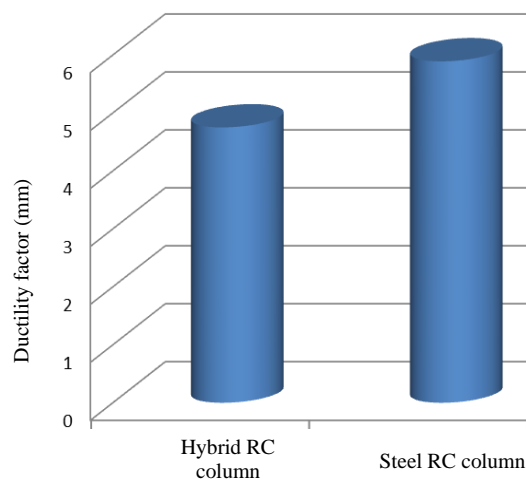


Fig. 11. Ductility factor for the simulated specimens.

#### 4.6 Reduction Factor

Under strong earthquakes, it is uneconomical to design the building for the seismic force considering the behavior is pure elastic. The building is expected to undergo the inelastic deformations with extending the period of structure and associated reduced design force. The force reduction reflects this behavior and is used to scale down the response spectrum for pure elastic behavior. Hence, structure is designed for seismic force much less than what is expected under strong shaking if the structure were to remain linearly elastic. The reduction factor is defined as the ratio between the maximum lateral force which would develop in a structure, responding entirely linear elastic under the specified ground motion, to the lateral force which has been designed to withstand. The force reduction factor  $R$  is a factor intended to account for damping, overstrength, and the ductility inherent in the structural system at displacements great enough to surpass initial yield and approach the ultimate load displacement of the structural system.

In order to estimate the ductility modification factor for the GFRP-reinforced concrete columns, the actual strength-displacement response should be idealized with the linearly elastic-perfectly plastic curve. To generate the bilinear idealization, a well-defined explicit transition between the elastic and inelastic deformation must be clear to identify the elastic-plastic transition point. In addition, the maximum deformation limit should be identified. The authors adopted the equivalent energy elastic-plastic method for bilinear idealization [29]. In calculation the force reduction factors the maximum drift ratio was set equal to 2.5% according to the NBCC [25]. Following this methodology, the reduction factor was found to be equal to 3.7 for the steel RC column, while this value was found equal to 2.5. This is definitely promising results considering the use of hybrid reinforcement systems in the new moment resisting frames generation.

### 5. DISCUSSION AND CONCLUSIONS

This study aimed to provide insight into the potential of the implication steel with GFRP reinforcement to develop more ductile columns while still being recoverable after strong earthquakes. The target also included a preliminary estimation for the force reduction factor of concrete columns reinforced with hybrid (steel/GFRP) reinforcement. Based on the analysis of the numerical results, the following conclusions were drawn:

1. The damage control that has been recorded in the hybrid RC columns did not impair the walls' ability to dissipate energy or the ductility index.
2. The force modification factor was evaluated based on the idealized curve and conservatively found to be 2.5 for hybrid RC column.
3. The durability issue should be carefully checked for the proposed hybrid reinforcement configurations under different environmental conditions, such as chloride permeability, repeated freeze–thaw cycles, and various chemical environments.

### REFERENCES

- [1] M. Yunovich and N. G. Thompson, "Corrosion of highway bridges: economic impact and control methodologies," *American Concrete Institute (ACI)*, Vol. 25, no. 1, pp. 52-57, Jan 2003.
- [2] American Concrete Institute (ACI), "Guide for the design and construction of structural concrete reinforced with fiber-reinforced polymer (frp) bars," ACI 440.1R-15, 2015 Farmington Hills, MI.
- [3] Canadian Standards Association (CAN/CSA), "Design and construction of building components with fiber-reinforced polymers (S806-12)," Mississauga, (ON, Canada): CSA, 2012, pp. 208.
- [4] A. Arafa, A. Farghaly, B. Benmokrane, "Experimental behavior of gfrp-reinforced concrete squat walls subjected to simulated earthquake load," *Journal of Composite for Construction*, 22(2), 2018a.
- [5] S. K. Ghomi and E. El-Salakawy, "Seismic behavior of exterior gfrp-rc beam–column connections: analytical study," *Journal of Composites for Construction*, vol. 22, no. 4, pp. 04018022, 2018.
- [6] E. El-Salakawy, B. Benmokrane, A. El-Ragaby, and D. Nadeau, "Field investigation on the first bridge deck slab reinforced with glass FRP bars constructed in Canada," *Journal of composites for construction*, vol. 9, no. 6, pp. 470-479, 2005.
- [7] B. Benmokrane, E. El-Salakawy, A. El-Ragaby, and S. El-Gamal, "Performance evaluation of innovative concrete bridge deck slabs reinforced with fiber-reinforced-polymer bars," *Canadian Journal of Civil Engineering*, vol. 34, no. 3, pp. 298-310, 2007.
- [8] A. Ehab, F. Settecesi, and B. Benmokrane, "Construction and testing of GFRP steel hybrid-reinforced concrete bridge-deck slabs of Sainte-Catherine overpass bridges," *Journal of Bridge Engineering*, vol. 19, no. 6, pp. 0401401, 2014.
- [9] H. Fukuyama, Y. Masuda, Y. Sonobe, M. Tanigaki, "Structural performances of concrete frame reinforced with FRP reinforcement," In 2nd international RILEM Symposium, Non-Metallic (FRP) Reinforcement for Concrete Structures, Ghent, Belgium: Chapman & Hall, pp. 275–86, 1995.
- [10] M. Hasaballa and E. El-Salakawy, "Shear capacity of exterior beam-column joints reinforced with GFRP bars and stirrups," *J Compos Constr*, vol. 20, no. 2, pp. 04015047, 2016.
- [11] D. Palermo, F. J. Vecchio, and H. Solanki, "Behavior of three-dimensional reinforced concrete shear walls," *ACI Structural Journal*, vol. 99, no. 1, pp. 81-89, 2002.
- [12] M. L. Nehdi and A. M. Said, "Behaviour of RC beam-column joints with hybrid reinforcement under simulated earthquake loading," 7th International Conference on Multipurpose High-Rise Towers and Tall Buildings, 2005.

- [13] A. Arafa, A. E. Shoeib, and S. Y Dandrawy, "Behavior of hybrid steel/gfrp reinforced columns under lateral cyclic loading: a numerical study," *Sohag Engineering Journal*, 1(1), pp.110-121,2021.
- [14] A. M. A. Ibrahim, Z. Wu, M. F. M. Fahmy, D. Kamal, "Experimental study on cyclic response of concrete bridge columns reinforced by steel and basalt frp reinforcements," *J Compos Constr*, Vol. 20, pp. 04015062,2016.
- [15] F. Bencardino, A. Condello, L. Ombres, "Numerical and analytical modeling of concrete beams with steel, FRP and hybrid FRP-steel reinforcements," *Compos Struct*, Vol. 140, pp. 53–65,2016.
- [16] R. Qin, A. Zhou, D. Lau, "Effect of reinforcement ratio on the flexural performance of hybrid frp reinforced concrete beams," *Compos B Eng*, Vol. 9, pp. 108-200,2017.
- [17] M. G. El-shamandy, A. S. Farghaly, and B. Benmokrane, "Experimental behavior of glass fiber-reinforced polymer-reinforced concrete columns under lateral cyclic load," *ACI Structural Journal*, vol. 115, no. 2, pp. 337-349, 2018.
- [18] D. Palermo and F. J. Vecchio, "Simulation of cyclically loaded concrete structures based on the finite-element method." *Journal of Structural Engineering*, vol. 133, no. 5, pp. 728-738, 2007.
- [19] Hognestad and Eivind, "Study of combined bending and axial load in reinforced concrete members," University of Illinois at Urbana Champaign, College of Engineering, Engineering Experiment Station, 1951.
- [20] B. D. Scott, R. Park and M. J. N. Priestley, "Stress-strain behavior of concrete confined by overlapping hoops at low and high strain rates," *J.ACI Struct.*, vol. 79, no. 1, pp. 13–27,1982.
- [21] P. S. Wong and F. J. Vecchio, "VecTor 2 & formworks user's manuals," Toronto, ON, Canada: Department of Civil Engineering, *University of Toronto*, pp. 213, 2002.
- [22] E. C. Bentz, "Sectional analysis of reinforced concrete members," Ph.D. Thesis, Department of Civil Engineering, University of Toronto, pp. 310, 2000.
- [23] H. Kupfer, H. K. Hilsdorf, and H. Rusch, "Behavior of concrete under biaxial stresses," *Journal proceedings*, Vol. 66, No. 8., pp. 656-666, 1969.
- [24] NBCC, "National Building Code of Canada," *National Research Council of Canada*," Ottawa, Ontario,2010.
- [25] X. G. He, and A. K. H. Kwan, " Modeling dowel action of reinforcement bars for finite element analysis of concrete structures," *Computers & Structures*, vol. 79, no. 6, pp.595-604, 2001.
- [26] L. Vint, "Investigation of bond properties of glass fiber reinforced polymer (GFRP) bars in concrete under direct tension," Diss, 2012.
- [27] H. Kupfer, B. Helmut, and K. H. Gerstle, "Behavior of concrete under biaxial stresses," *Journal of the engineering mechanics division*, vol. 99, no. 4, pp. 853-866, 1973.
- [28] P. Ricci, G. M. Verderame, and G. Manfredi, "ASCE/SEI 41 provisions on deformation capacity of older-type reinforced concrete columns with plain bars," *Journal of Structural Engineering*, vol. 139, no. 12, pp. 04013014, 2013.
- [29] A. Hassanein, A. S. Farghaly, B. Benmokrane, "Experimental investigation: new ductility-based force modification factor recommended for concrete shear walls reinforced with glass fiber reinforced polymer bars," *ACI structural Journal*, Vol. 1, pp. 213-224,2019.